

# Biosignatures link microorganisms to iron mineralization in a paleoaquifer

Karrie A. Weber<sup>1,2\*</sup>, Trisha L. Spanbauer<sup>1†</sup>, David Wacey<sup>3,4</sup>, Matthew R. Kilburn<sup>3</sup>, David B. Loope<sup>2</sup>, and Richard M. Kettler<sup>2</sup>

<sup>1</sup>School of Biological Sciences, University of Nebraska, Lincoln, Nebraska 68588, USA

<sup>2</sup>Department of Earth and Atmospheric Sciences, University of Nebraska, Lincoln, Nebraska 68583, USA

<sup>3</sup>Centre for Microscopy, Characterisation and Analysis, University of Western Australia, Crawley, WA 6009, Australia

<sup>4</sup>School of Earth and Environment, University of Western Australia, Crawley, WA 6009, Australia

## ABSTRACT

**Concretions, preferentially cemented masses within sediments and sedimentary rocks, are records of sediment diagenesis and tracers of pore water chemistry. For over a century, rinded spheroidal structures that exhibit an Fe(III) oxide-rich exterior and Fe-poor core have been described as oxidation products of Fe(II) carbonate concretions. However, mechanisms governing Fe(III) oxide precipitation within these structures remain an enigma. Here we present chemical and morphological evidence of microbial biosignatures in association with Fe(III) oxides in the Fe(III) oxide-rich rind of spheroidal concretions collected from the Jurassic Navajo Sandstone (southwest United States), implicating a microbial role in Fe biomineralization. The amount of total organic carbon in the exterior Fe(III) oxides exceeded measured values in the friable interior. The mean  $\delta^{13}\text{C}$  value of organic carbon from the Fe(III) oxide-cemented exterior,  $\delta^{13}\text{C}$  of  $-20.55\text{‰}$ , is consistent with a biogenic signature from autotrophic bacteria. Scanning electron micrographs reveal microstructures consistent with bacterial size and morphology, including a twisted-stalk morphotype that resembled an Fe(II)-oxidizing microorganism, *Gallionella* sp. Nanoscale associations of Fe, O, C, and N with bacterial morphotypes demonstrate microorganisms associated with Fe(III) oxides. Together these results indicate that autotrophic microorganisms were present during Fe(III) oxide precipitation and present microbial catalysis as a mechanism of Fe(III) oxide concretion formation. Microbial biosignatures in rinded Fe(III) oxide-rich concretions within an exhumed, Quaternary aquifer has broad implications for detection of life within the geological record on Earth as well as other Fe-rich rocky planets such as Mars, where both Fe(II) carbonate and Fe(III) oxide-rich concretions have been identified.**

## INTRODUCTION

Reduced organic carbon is the primary energy source for biological activity in many environments. However, in environments with limited organic carbon and light, alternative energy sources, such as Fe(II), must be available in order for life to persist. Since accumulation of abundant molecular oxygen ( $\text{O}_2$ ) in Earth's atmosphere during the Proterozoic, Fe(II) has nearly disappeared from continental and marine surficial systems (Walther, 2009). Thus, Fe(II)-rich water at near-neutral pH is restricted to low concentrations in most environments, with exceptions in highly reduced saturated soils, water, and subsurface sediments (Weber et al., 2006). These Fe(II)-bearing environments have been shown to support microbial life (Weber et al., 2006). Siderite or ankerite, common minerals in nonmarine sediments (Berner, 1981), could provide Fe(II) as an energy source for microbial metabolism as well as supply a source of inorganic carbon for fixation into organic carbon via autotrophic metabolisms. In the presence of  $\text{O}_2$ , dissolution of siderite is promoted by the production of acid

resulting from Fe(II) oxidation and precipitation of Fe(III) oxides (Duckworth and Martin, 2004). These reactions can occur abiotically, but are mediated by  $\text{O}_2$  concentrations. At low  $\text{O}_2$  concentrations, Fe(II)-oxidizing microorganisms can successfully outcompete abiotic mechanisms for available Fe(II) (Druschel et al., 2008; Neubauer et al., 2002) and catalyze Fe(II) oxidation. Metabolic activity also establishes and maintains a favorable geochemical environment in an oxic system (low dissolved  $\text{O}_2$ , 15–50  $\mu\text{M}$ , 0.45–1.5 mg/L) (Druschel et al., 2008; Emerson and Moyer, 1997; Sobolev and Roden, 2001). Microorganisms can establish a geochemical gradient at the interface between oxidizing groundwater and Fe(II) carbonate minerals inhabiting environments with low dissolved  $\text{O}_2$  concentrations. Thus, Fe(II) carbonate present in a saturated environment would provide necessary conditions for microaerophilic Fe(II)-oxidizing bacteria to persist and thrive.

Siderite identified on Fe(III) oxide-rich planets such as Earth and Mars (Michalski and Niles, 2010; Morris et al., 2010) is an alternative energy source for microbial life (Weber et al., 2006). Subsequent Fe(II) oxidation would result in the formation of Fe(III) oxide-rich formations including Fe(III) oxide cements. Fe(III)

oxide cements in nonmarine sandstones occur as a variety of bands and concretions including spheroids, joint-associated boxes, and pipes (Loope et al., 2011). While these concretions are widespread, mechanisms underpinning the formation of an Fe-rich exterior and Fe-depleted core are poorly understood. Recently, rinded Fe(III) oxide concretions in the Navajo Sandstone (southwest United States) have received great interest (Chan et al., 2004; Loope et al., 2010; Parry, 2011; Potter et al., 2011), not least due to their potential use as analogues for Fe(III) oxide-rich concretions observed on Mars (Chan et al., 2004; Potter et al., 2011).

These Fe(III) oxide-rich concretions formed in the Jurassic Navajo Sandstone subsequent to incision by the Colorado River (Loope et al., 2010). Most previous studies have interpreted spheroidal iron oxide concretions to be abiotic oxidation products of dissolved Fe(II) mixing with oxic fluids resulting in spheroid formation without a structural precursor (Chan et al., 2004; Potter et al., 2011; Souza-Egipsy et al., 2006). An alternative to this mixing model uses Fe(II) carbonate, including siderite, as the initial Fe(II) source and structural precursor of rinded spheroids (Loope et al., 2010). This structural precursor is consistent with prior descriptions of iron and carbonate concretion formation (Curtis and Coleman, 1986), rather than published descriptions as products of mixing of reduced and oxidizing fluids (Beitler et al., 2005; Chan et al., 2004). Evidence of the carbonate precursor is provided by the presence of rhombic Fe(III) oxide pseudomorphs after siderite (Loope et al., 2011). The Fe-rich spheroidal concretions are composed of an amorphous Fe(III) oxide, goethite, and hematite (Potter et al., 2011) that surround the iron-poor sand interior. It has been hypothesized that microorganisms played a role in formation of rinded Fe(III) oxide concretions (Souza-Egipsy et al., 2006; Loope et al., 2010), but evidence of past microbial life has eluded other investigators (Souza-Egipsy et al., 2006). We initiated an investigation to identify microbial biosignatures as a first test of our hypothesis that bacteria were present in spheroidal concretions during Fe mineralization.

## RESULTS AND DISCUSSION

Intact spheroidal Fe(III) oxide concretions of varying sizes <5 cm (Fig. DR1 in the GSA

\*E-mail: kweber2@unl.edu.

†Current address: Department of Earth and Atmospheric Sciences, University of Nebraska, Lincoln, Nebraska 68583, USA.

Data Repository<sup>1</sup>) were collected from outcrops of light-colored Navajo Sandstone at the southern margin of Spencer Flat in south-central Utah (Fig. DR2). Fe(III) oxides in the rind were separated from the interior prior to carbon and nitrogen analysis. Carbon and nitrogen concentrations in the Fe(III) oxide-rich rind (C, 0.06% ± 0.003%; N, 0.006% ± 0.0002%) were greater than those measured in the interior of concretions (C, 0.009% ± 0.0001%; N, 0.003% ± 0.0005%). These data are consistent with biogenic compounds in the rind. The mean  $\delta^{13}\text{C}$  content, organic carbon and carbonate, of triplicate Fe(III) oxide-rich rind samples revealed a value of  $-7.05\text{‰} \pm 0.75\text{‰}$  (Table DR1 in the Data Repository). This value suggests that carbon had an abiotic origin. However, removal of carbonates from the Fe(III) oxide-rich samples (in situ acidification with 6N HCl; Larson et al., 2008) revealed a  $\delta^{13}\text{C}$  value for organic carbon of  $-20.55\text{‰} \pm 2.69\text{‰}$  (Table DR1), consistent with  $\delta^{13}\text{C}$  depletion biosignatures for bacteria using the Calvin cycle for CO<sub>2</sub> fixation (Zerkle et al., 2005) and recently reported values for neutrophilic Fe(II)-oxidizing bacteria, including *Gallionella ferruginea* (Kennedy et al., 2010). *Gallionella ferruginea* is a common Fe(II)-oxidizing microorganism capable of autotrophic growth (fixing CO<sub>2</sub> into organic carbon) (Hallbeck and Pedersen, 1991) and is frequently identified at redox interfaces where Fe(II) meets an oxic environment (Hallbeck and Pedersen, 2005).

In an effort to identify and verify the presence of microorganisms preserved in Fe(III) oxide concretions, we examined intergranular pore spaces along inner margins of Fe(III) oxide rinds of small (<1 cm) concretions using field emission scanning electron microscopy (FE-SEM) (Fig. 1A). Microscopic analyses revealed morphological microstructures consistent with microorganisms (width 0.25–4  $\mu\text{m}$ , varying length >1.5  $\mu\text{m}$ ). A diversity of morphotypes were observed, including bacillus-like (0.6  $\mu\text{m}$  × 3  $\mu\text{m}$ ; Fig. 1B), filamentous (0.2  $\mu\text{m}$  × <3.5  $\mu\text{m}$ ; Fig. 1C), and twisted-stalk (<0.4  $\mu\text{m}$  × >60  $\mu\text{m}$ ; Fig. 1D). Although bacteria cannot generally be taxonomically identified solely based on morphology and size, twisted-stalk morphology (Fig. 1D) is unique to certain Fe(II)-oxidizing bacteria, *Gallionella* sp. (Chan et al., 2009; Ferris et al., 1999; Hallberg and Ferris, 2004) and *Marinobacter* sp. (Chan et al., 2011). The most abundant morphotype observed throughout the concretions was the bacillus-like structures protruding from the sur-

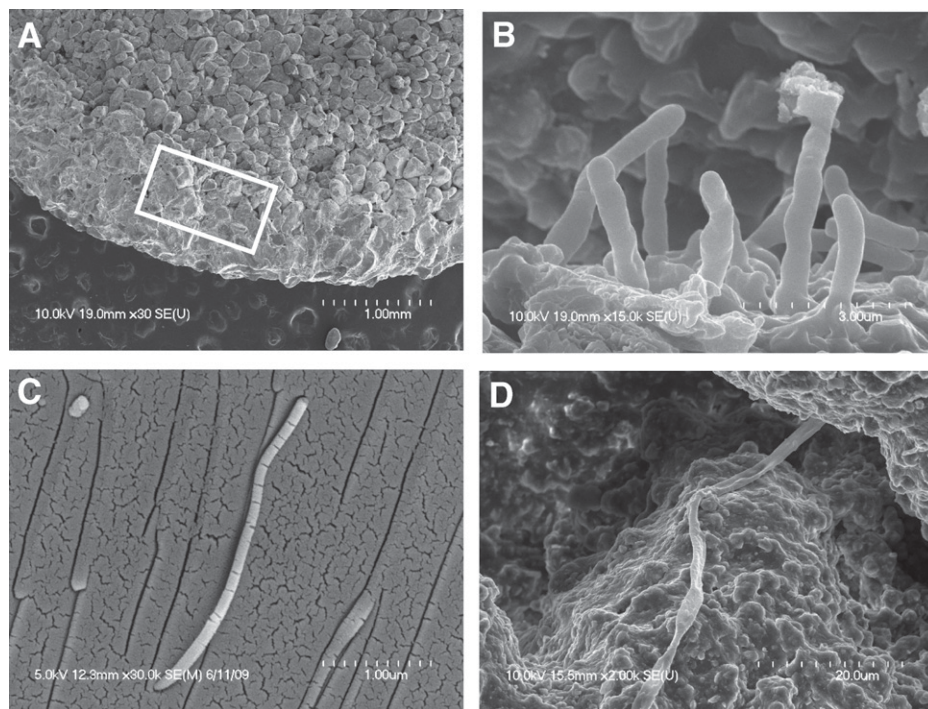


**Figure 1.** Field emission scanning electron micrographs of microbial fossils in Fe(III) oxide rind of a spheroidal iron oxide concretion collected from Navajo Sandstone (southwest United States). Images shown were acquired from numerous specimens of small (1 cm) spheroidal concretions. **A:** The interface between Fe(III) oxide rinds and bleached sandstone toward the interior was the region targeted for analyses (denoted by the white box). Multiple microbial morphotypes were identified consistent with rod-shaped microorganisms (**B**), filamentous microorganisms (**C**), and a twisted stalk similar to well-characterized, neutrophilic, Fe(II)-oxidizing bacteria such as *Gallionella* sp. (**D**).

faces of sand grains (Fig. 1B). The abundance and close association of these microorganisms resembles a biofilm. The bacillus-like morphotypes were further analyzed by energy-dispersive X-ray spectroscopy (EDS). The structures were largely composed of carbon, oxygen, and iron (Fig. DR3). Carbon was localized to the bacillus-like structures (Fig. DR3).

Nanoscale geochemical analysis using NanoSIMS further showed an intimate association of bacterial morphotypes with carbon, oxygen, nitrogen, and iron (measured as <sup>12</sup>C, <sup>16</sup>O, <sup>12</sup>C<sup>14</sup>N, and <sup>56</sup>Fe<sup>16</sup>O, respectively). In order to distinguish true biological material from the resin in which the sample was embedded, a number of replicate images of resin were analyzed and CN<sup>-</sup>/C<sup>-</sup> ratios were calculated (Wacey et al., 2010). Mean CN<sup>-</sup>/C<sup>-</sup> ratios associated with resin were 0.53 ± 0.3 (n = 40). In contrast, mean CN<sup>-</sup>/C<sup>-</sup> ratios associated with areas of iron oxide were 2.10 ± 0.3 (n = 30), a clear increase from those found in resin. This result was consistent across numerous areas in the iron oxide rind. Hence, it was possible to threshold the NanoSIMS images (Fig. 2) to remove the background signal and highlight biological material associated with iron oxides. Structures similar to microbial fossils imaged by SEM were also observed in NanoSIMS images (Fig. 2, white circles). They were par-

ticularly common at edges of Fe(III) oxide-rich areas. Here bacillus-like microorganisms were identified, consistent with the most common microbial morphology observed by SEM. These structures show elevated CN<sup>-</sup>/C<sup>-</sup> ratios together with FeO<sup>-</sup>, further demonstrating a relationship between microbial morphology, Fe(III) oxide minerals, and nitrogen-rich organic material (Fig. 2). Together these data demonstrated morphologies consistent with bacteria, including a known Fe(II)-oxidizing microorganism, and Fe associated with fossil structures, thus indicating that bacteria were present during iron mineralization in the paleoaquifer.

A conceptual biogeochemical/geomicrobiological model detailing the role of microorganisms catalyzing the oxidative dissolution of Fe(II) carbonate and the biomineralization of iron to form Fe(III) oxide concretions with a bleached interior (Fig. 3) was constructed based on new data together with previously published data (Loope et al., 2010, 2011). The available energy (Fe(II)) and carbon (carbonate) present in the precursor plus pore fluids containing dissolved O<sub>2</sub> (electron acceptor) could have supported an iron-oxidizing microbial community. When siderite concretions were exposed to oxidizing groundwater (Loope et al., 2010), a redox interface developed between oxic groundwater and Fe(II) carbonate. These conditions created

<sup>1</sup>GSA Data Repository item 2012205, supplemental information including methods,  $\delta^{13}\text{C}$  data, Fe(III) oxide-rich concretion images, map, and FE-SEM image with EDS data, is available online at [www.geosociety.org/pubs/ft2012.htm](http://www.geosociety.org/pubs/ft2012.htm), or on request from [editing@geosociety.org](mailto:editing@geosociety.org) or Documents Secretary, GSA, P.O. Box 9140, Boulder, CO 80301, USA.

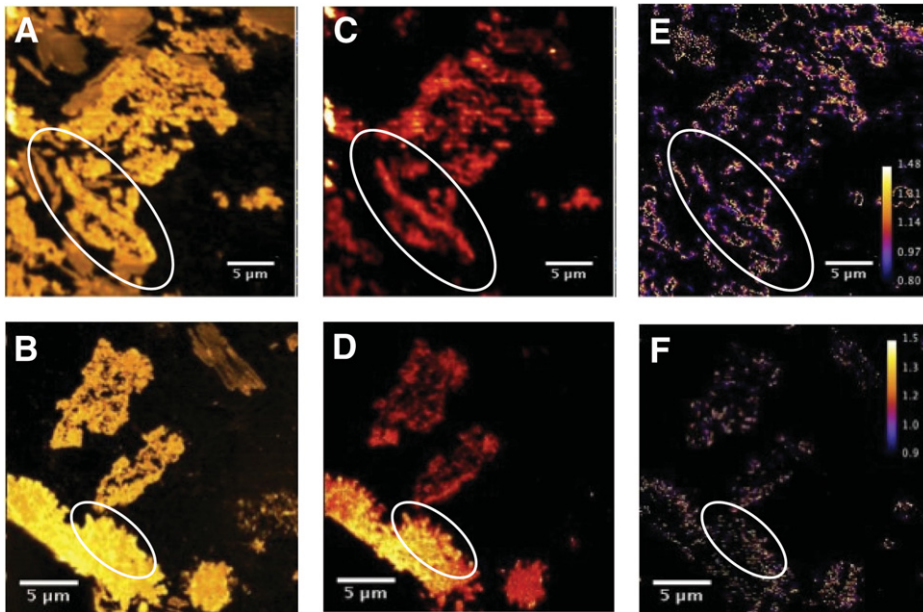


**Figure 2.** NanoSIMS analysis of a spheroidal iron oxide concretion cross section. Images depict mapped regions of  $^{16}\text{O}^-$  (A and B),  $^{56}\text{Fe}^{16}\text{O}^-$  (C and D), and  $^{12}\text{C}^{14}\text{N}^-$  (E and F) collected from two areas located in pore spaces at the interface between Fe(III) oxides and bleached sandstone interior. Morphological structures resembling microorganisms observed under field emission scanning electron microscopy (FE-SEM) are denoted by white circles. A, C, and E resemble a filament similar to Figure 1C, and B, D, and F depict rod-shaped structures protruding from the quartz surface, similar to Figure 1B. Brighter regions in the  $^{16}\text{O}^-$  and  $^{56}\text{Fe}^{16}\text{O}^-$  maps indicate higher ion intensities. The  $^{12}\text{C}^{14}\text{N}^-/^{12}\text{C}^-$  images show areas containing organic matter of likely biological origin, with ratios between  $\sim 0.8$  and 1.5, and have been corrected to exclude any signal from resin. Organic matter was directly associated with iron minerals that morphologically resemble bacteria (white circles).

an environment for neutrophilic Fe(II)-oxidizing microorganisms to proliferate, fixing  $\text{CO}_2$  into organic carbon, thereby fractionating carbon. Acid generated as a result of both biotic and abiotic Fe(II) oxidation / Fe(III) oxide precipitation in the oxic environment facilitated dissolution of Fe(II) carbonate cement (Fig. 3). Circumneutral pH was maintained by carbonate equilibrium allowing aqueous Fe(II) to diffuse from the interior toward the exterior and generated an Fe(II) and  $\text{O}_2$  redox interface (Fig. 3). Iron biomineralization occurred at the redox interface. This self-promoting process continued until Fe(II) carbonates were completely dissolved or conditions precluded microbial metabolism (Fig. 3). The formation of hydrous ferric iron oxide minerals such as ferrihydrite, lepidocrocite, and goethite (Potter et al., 2011) is consistent with previously published data describing microbial Fe(III) oxide formation (Chan et al., 2009, 2011) and preservation of metastable phases such as ferrihydrite (Kennedy et al., 2004). Oxidative, microbially catalyzed dissolution of precursor siderite concretions thus offers an alternative hypothesis for the origin of rinded Fe(III) oxide-cemented structures originating in nonmarine sandstones.

Here we presented the first example of Fe-coated microbial fossils in spheroidal Fe(III) oxide-rich concretions with an Fe-poor core.

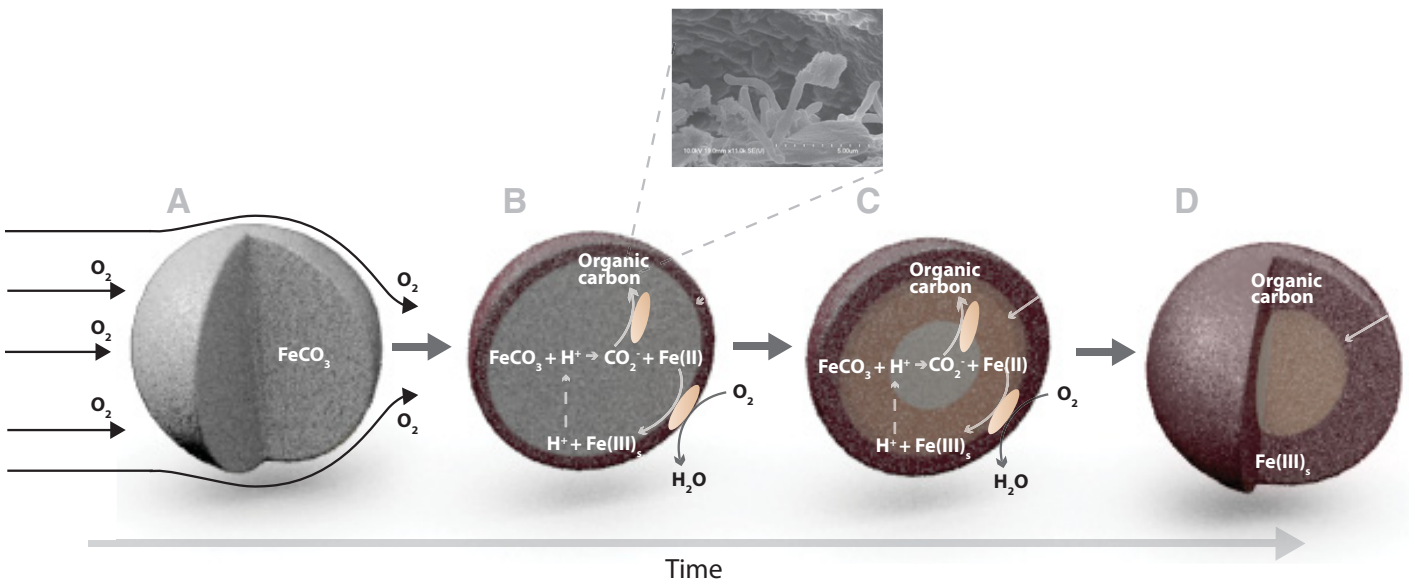


**Figure 3.** Conceptual model of oxidative iron biomineralization of Fe-rich concretions in an aquifer system. **A:** Oxic fluids moving (gray arrows denote flow) through a sedimentary environment (i.e., sandstone matrix) carrying  $\text{O}_2$ , thus exposing siderite concretions to an oxidizing environment. **B:** Microorganisms transformed the Fe(II) carbonate concretions through the oxidation of Fe(II) coupled to the reduction of  $\text{O}_2$  (reaction noted by placement of a rod-shaped bacterium) at the exterior of the Fe(III) oxide concretion. This produced protons (acidity) and precipitation of iron oxides:  $4\text{Fe(II)} + \text{O}_2 + 10\text{H}_2\text{O} \rightarrow 4\text{Fe(OH)}_3 + 8\text{H}^+$  (Fe(III)<sub>s</sub> denotes solid-phase Fe oxides). Acid promoted Fe(II) carbonate dissolution and release of aqueous Fe(II) and dissolved carbonate species:  $\text{H}^+ + \text{FeCO}_3 \rightarrow \text{Fe(II)} + \text{HCO}_3^-$  (dashed line denotes diffusion of  $\text{H}^+$ , solid arrows denote reaction progress). Dissolved Fe(II) and carbonate/ $\text{CO}_2$  species freely diffused toward the exterior of the concretion. Fe(II) was oxidized at the redox interface and carbonate/ $\text{CO}_2$  was autotrophically converted into organic carbon by iron-oxidizing microorganisms (reaction noted by placement of a rod-shaped bacterium). SEM image collected at the interface of Fe(III) oxides and interior as denoted in Figure 1 illustrates placement of microorganisms in the Fe concretions. **C:** Continual microbial activity resulted in precipitation of Fe(III) oxides and inward growth of the outer rind. **D:** The dissolved Fe(II) diffused toward the exterior until Fe(II) carbonate was completely dissolved and oxidized, leaving an Fe(III) oxide rind and bleached sandstone interior. Gray denotes Fe(II) carbonate, and brownish-red denotes solid-phase Fe(III) oxides.

The direct association of Fe(III) oxides with microbial fossils implicates microorganisms in Fe(III) oxide biomineralization during the oxidative dissolution of Fe(II) carbonate. This process is not limited to spheroidal concretions; we have identified various structures within the Navajo Sandstone, such as pipe-like concretions and joint-associated boxworks (Loope et al., 2011, 2012), that similarly display an Fe(III) oxide-rich rind with an Fe-poor core. This process is likely operative in modern saturated environments including aquifers on Earth as well as on Fe-rich rocky planets bearing siderite such as Mars (Michalski and Niles, 2010). Iron oxide concretions with an Fe(III) oxide-rich exterior and an iron-poor core therefore offer a macroscopic target in the search for life on Earth as well as Mars.

#### ACKNOWLEDGMENTS

This study was carried out in Grand Staircase-Escalante National Monument with cooperation of the Bureau of Land Management and assistance of C. Shelton and A. Titus. We are grateful to C. Okafor, C. McFadden, A. Shultis, D. Snow, H. Chen, and K. Sun for assistance with sample preparation and analyses. The authors acknowledge facilities, scientific, and technical assistance of the Australian Microscopy and Microanalysis Research Facility at the Centre for Microscopy, Characterisation and Analysis for NanoSIMS analysis at UWA, facility funded by the University, State, and Commonwealth Governments. This research was supported by the UNL Research Office and Nebraska Tobacco Settlement Fund. Manuscript preparation was supported by NSF ADVANCE-Nebraska grant 0811250.

#### REFERENCES CITED

- Beitler, B., Parry, W.T., and Chan, M.A., 2005, Fingerprints of fluid flow: Chemical diagenetic history of the Jurassic Navajo Sandstone, southern Utah, U.S.A.: *Journal of Sedimentary Research*, v. 75, p. 547–561, doi:10.2110/jsr.2005.045.
- Berner, R.A., 1981, A new geochemical classification of sedimentary environments: *Journal of Sedimentary Research*, v. 51, p. 359–365.
- Chan, C.S., Fakra, S.C., Edwards, D.C., Emerson, D., and Banfield, J.F., 2009, Iron oxyhydroxide mineralization on microbial extracellular polysaccharides: *Geochimica et Cosmochimica Acta*, v. 73, p. 3807–3818, doi:10.1016/j.gca.2009.02.036.
- Chan, C.S., Fakra, S.C., Emerson, D., Fleming, E.J., and Edwards, K.J., 2011, Lithotrophic iron-oxidizing bacteria produce organic stalks to control mineral growth: Implications for biosignature formation: *ISME Journal*, v. 5, p. 717–727, doi:10.1038/ismej.2010.173.
- Chan, M.A., Beitler, B., Parry, W.T., Ormo, J., and Komatsu, G., 2004, A possible terrestrial analogue for haematite concretions on Mars: *Nature*, v. 429, p. 731–734, doi:10.1038/nature02600.
- Curtis, C.D., and Coleman, M.L., 1986, Controls on the precipitation of early diagenetic calcite, dolomite, and siderite concretions in complex depositional sequences, in Gautier, D.L., ed., *Roles of organic matter in sediment diagenesis: Society of Economic Paleontologists and Mineralogists Special Publication 38*, p. 23–33.
- Druschel, G.K., Emerson, D., Sutka, R., Suchecki, P., and Luther, G.W., III, 2008, Low-oxygen and chemical kinetic constraints on the geochemical niche of neutrophilic iron(II) oxidizing microorganisms: *Geochimica et Cosmochimica Acta*, v. 72, p. 3358–3370, doi:10.1016/j.gca.2008.04.035.
- Duckworth, O.W., and Martin, S.T., 2004, Role of molecular oxygen in the dissolution of siderite and rhodochrosite: *Geochimica et Cosmochimica Acta*, v. 68, p. 607–621, doi:10.1016/S0016-7037(03)00464-2.
- Emerson, D., and Moyer, C.L., 1997, Isolation and characterization of novel iron-oxidizing bacteria that grow at circumneutral pH: *Applied and Environmental Microbiology*, v. 63, p. 4784–4792.
- Ferris, F.G., Konhauser, K.O., Lyven, B., and Pedersen, K., 1999, Accumulation of metals by bacteriogenic iron oxides in a subterranean environment: *Geomicrobiology Journal*, v. 16, p. 181–192, doi:10.1080/014904599270677.
- Hallbeck, L., and Pedersen, K., 1991, Autotrophic and mixotrophic growth of *Gallionella ferruginea*: *Journal of General Microbiology*, v. 137, p. 2657–2661.
- Hallbeck, L.E.L., and Pedersen, K., 2005, *Genus I. Gallionella Ehrenberg 1838, 166<sup>AL</sup>*, in Garrity, G., et al., eds., *Bergey's manual of systematic bacteriology*, volume two: *The Proteobacteria*, part C: *The Alpha-, Beta-, Delta-, and Epsilon-proteobacteria*: New York, Springer, p. 880–886.
- Hallberg, R., and Ferris, F.G., 2004, Biomineralization by *Gallionella*: *Geomicrobiology Journal*, v. 21, p. 325–330, doi:10.1080/01490450490454001.
- Kennedy, C.B., Scott, S.D., and Ferris, F.G., 2004, Hydrothermal phase stabilization of 2-line ferrihydrite by bacteria: *Chemical Geology*, v. 212, p. 269–277, doi:10.1016/j.chemgeo.2004.08.017.
- Kennedy, C.B., Gault, A.G., Fortin, D., Clark, I.D., Pedersen, K., Scott, S.D., and Ferris, F.G., 2010, Carbon isotope fractionation by circumneutral iron-oxidizing bacteria: *Geology*, v. 38, p. 1087–1090, doi:10.1130/G30986.1.
- Larson, T.E., Heikoop, J.M., Perkins, G., Chipera, S.J., and Hess, M.A., 2008, Pretreatment technique for siderite removal for organic carbon isotope and C:N ratio analysis in geological samples: *Rapid Communications in Mass Spectrometry*, v. 22, p. 865–872, doi:10.1002/rcm.3432.
- Loope, D.B., Kettler, R.M., and Weber, K.A., 2010, Follow the water: Connecting a CO<sub>2</sub> reservoir and bleached sandstone to iron-rich concretions in the Navajo Sandstone of south-central Utah, USA: *Geology*, v. 38, p. 999–1002, doi:10.1130/G31213.1.
- Loope, D.B., Kettler, R.M., and Weber, K.A., 2011, Morphologic clues to the origins of iron oxide-cemented spheroids, boxworks, and pipelike concretions, Navajo Sandstone of south-central Utah, U.S.A.: *Journal of Geology*, v. 119, p. 505–520, doi:10.1086/661110.
- Loope, D.B., Kettler, R.M., Weber, K.A., Hinrichs, N.L., and Burgess, D.T., 2012, Rinded iron-oxide concretions: Hallmarks of altered siderite masses of both early and late diagenetic origin: *Sedimentology*, doi:10.1111/j.1365-3091.2012.01325.x.
- Michalski, J.R., and Niles, P.B., 2010, Deep crustal carbonate rocks exposed by meteor impact on Mars: *Nature Geoscience*, v. 3, p. 751–755, doi:10.1038/ngeo971.
- Morris, R.V., Ruff, S.W., Gellert, R., Ming, D.W., Arvidson, R.E., Clark, B.C., Golden, D.C., Siebach, K., Klingelhofer, G., Schroder, C., Fleischer, I., Yen, A.S., and Squyres, S.W., 2010, Identification of carbonate-rich outcrops on Mars by the Spirit rover: *Science*, v. 329, p. 421–424, doi:10.1126/science.1189667.
- Neubauer, S.C., Emerson, D., and Magonigal, J.P., 2002, Life at the energetic edge: Kinetics of circumneutral iron oxidation by lithotrophic iron-oxidizing bacteria isolated from the wetland-plant rhizosphere: *Applied and Environmental Microbiology*, v. 68, p. 3988–3995, doi:10.1128/AEM.68.8.3988-3995.2002.
- Parry, W.T., 2011, Composition, nucleation, and growth of iron oxide concretions: *Sedimentary Geology*, v. 233, p. 53–68, doi:10.1016/j.sedgeo.2010.10.009.
- Potter, S.L., Chan, M.A., Petersen, E.U., Dyar, M.D., and Sklute, E., 2011, Characterization of Navajo Sandstone concretions: Mars comparison and criteria for distinguishing diagenetic origins: *Earth and Planetary Science Letters*, v. 301, p. 444–456, doi:10.1016/j.epsl.2010.11.027.
- Sobolev, D., and Roden, E.E., 2001, Suboxic deposition of ferric iron by bacteria in opposing gradients of Fe(II) and oxygen at circumneutral pH: *Applied and Environmental Microbiology*, v. 67, p. 1328–1334, doi:10.1128/AEM.67.3.1328-1334.2001.
- Souza-Egipsy, V., Ormo, J., Bowen, B.B., Chan, M.A., and Komatsu, G., 2006, Ultrastructural study of iron oxide precipitates: Implications for the search for biosignatures in the Meridiani hematite concretions, Mars: *Astrobiology*, v. 6, p. 527–545, doi:10.1089/ast.2006.6.527.
- Wacey, D., Gleeson, D., and Kilburn, M.R., 2010, Microbialite taphonomy and biogenicity: New insights from NanoSIMS: *Geobiology*, v. 8, p. 403–416, doi:10.1111/j.1472-4669.2010.00251.x.
- Walther, J.V., 2009, *Essentials of geochemistry*: Sudbury, Massachusetts, Jones and Bartlett, 797 p.
- Weber, K.A., Achenbach, L.A., and Coates, J.D., 2006, Microorganisms pumping iron: Anaerobic microbial iron oxidation and reduction: *Nature Reviews Microbiology*, v. 4, p. 752–764, doi:10.1038/nrmicro1490.
- Zerkle, A.L., House, C.H., and Brantley, S.L., 2005, Biogeochemical signatures through time as inferred from whole microbial genomes: *American Journal of Science*, v. 305, p. 467–502.

Manuscript received 28 November 2011  
 Revised manuscript received 8 March 2012  
 Manuscript accepted 12 March 2012

Printed in USA